
scale factors to $\beta = 0.131$, $\alpha = 0.131$ and $\gamma = 0.014$ yielded acceptable estimates of thrombin-binding affinity as well.²⁵ In addition, the extended linear response equation has potential for predictions of other properties important for pharmacological activity, such as the estimation of ligand lipophilicity.²⁴ It has been observed that the contribution of the Δ SASA term is often nearly constant, so the case in which the simple addition of a constant improves the fit has also been considered [eq (3)].^{20,25}

$$\Delta G_b = \beta \langle \Delta E^{\text{Coulomb}} \rangle + \alpha \langle \Delta E^{\text{Lennard-Jones}} \rangle + \gamma \langle \Delta \text{SASA} \rangle \quad (2)$$

$$\Delta G_b = \beta \langle \Delta E^{\text{Coulomb}} \rangle + \alpha \langle \Delta E^{\text{Lennard-Jones}} \rangle + \gamma \quad (3)$$

In contrast to most proteins studied previously with this technique, FKBP12 has a distinctly hydrophobic binding pocket lined with aromatic residues, and only two intermolecular hydrogen bonds are observed in the crystal structure of inhibitor **4** with the protein.⁹ Consequently, it was expected that the electrostatic behavior of these molecules might deviate from linear response and that the van der Waals contributions to binding might be larger than previously observed for other systems. To determine the suitability of the linear response approximation for binding to FKBP12, MC simulations of the bound and unbound states for all 11 inhibitors in Table 1 were performed.

Computational Details

The modeling strategy employed here was consistent with the FEP study described previously,¹⁶ based on the **4**-FKBP12 crystal structure (1FKG)⁹ and the OPLS force field.^{26–28} (A full listing of parameters for these molecules may be found in ref 29) The first five inhibitors were easily built from **4**. Atoms of the 1-phenyl substituent were simply removed to obtain **2**, and for compound **1**, a united-atom cyclohexyl group³⁰ was positioned in the plane of the original 3-phenyl ring. The vinyl group of **3** was also represented with united-atom parameters and was positioned at the minimum of the CH₃–C–CH=CH₂ torsional energy profile (180.0°) and aligned with an edge of the 1-phenyl ring of **4**.²⁹ One side of this ring was within 3.2 Å of His⁸⁷ and Tyr⁸², while the other was positioned more than 3.5 Å from Phe⁴⁶ and Glu⁵⁴. Accordingly, the orientation which maximized hydrophobic contact between the protein and **3** was chosen. Inhibitor **5** incorporated the crystal structure orientations of the cyclohexyl and *tert*-pentyl groups from **5**-FKBP12 (1FKH).⁹ In **1** and **5**, the cyclohexyl groups were treated as rigid units, as were all ligand and protein aromatic groups. It was thought that the conformational flexibility within the rings of these substituents would be less important to binding than the overall flexibility of the ligand, and thus sampling was focused accordingly. Starting geometries for the unbound ligand simulations were taken from these initial bound conformations.

All simulations were performed using the MCPRO program and Monte Carlo configurational sampling.³¹

The ligands and protein–ligand complexes were solvated with 22 Å spheres of TIP4P water molecules. First, 1×10^6 (1 *M*) configurations of water-only equilibration with preferential sampling of molecules close to the inhibitor was performed, followed by 16 *M* configurations of sampling of the entire system with all solvent molecules sampled uniformly. Next, data was collected for 8 *M* configurations averaged in blocks of 2×10^5 configurations. To ensure convergence, averaging for all unbound ligands was extended to 16 *M* configurations.

To obtain protein-bound structures of **6** and **7**, the final conformations of **4** and **5** above were epimerized within the FKBP12 binding pocket via a slow perturbation protocol. Eight sequential double-wide windows with $\Delta\lambda = 10.0625$ were used. In each window, 4 *M* configurations were sampled to slowly transform between the two ligands in an energetically reasonable way. This procedure was repeated with the free ligands in solution. The simulations of ligands **8–11** were started from the final structures of FEP simulations reported previously.^{16,29} In each case, energy components were averaged over 8 *M* (bound) and 16 *M* (unbound) configurations of the system.

As was mentioned above, the initial structure for **2** had been generated from the bound conformation of **4** with the 1-phenyl atoms removed. Following an FEP calculation from **4** to **2**, further sampling was carried out within the first windows of both a phenyl→pyridyl FEP¹⁶ and a carbonyl→hydroxyl FEP.²⁹ The final conformations of these windows were then used to start two additional linear response MC simulations, **2a** and **2b**, respectively. These additional data points provide one gauge of precision.

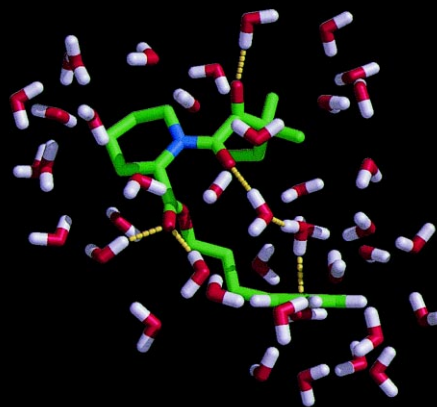
Solvent-accessible surface areas for the ligands in both aqueous and protein environments were calculated using the SAVOL2 program.³² This algorithm has been incorporated into MCPRO, and the necessary atomic radii are calculated from the corresponding OPLS σ parameters via $1/2 (2^{1/6}\sigma)$. Using the standard solvent radius for water, 1.4 Å, the SASAs of the ligands were calculated for the structure at the end of each block of MC configurations and were averaged.

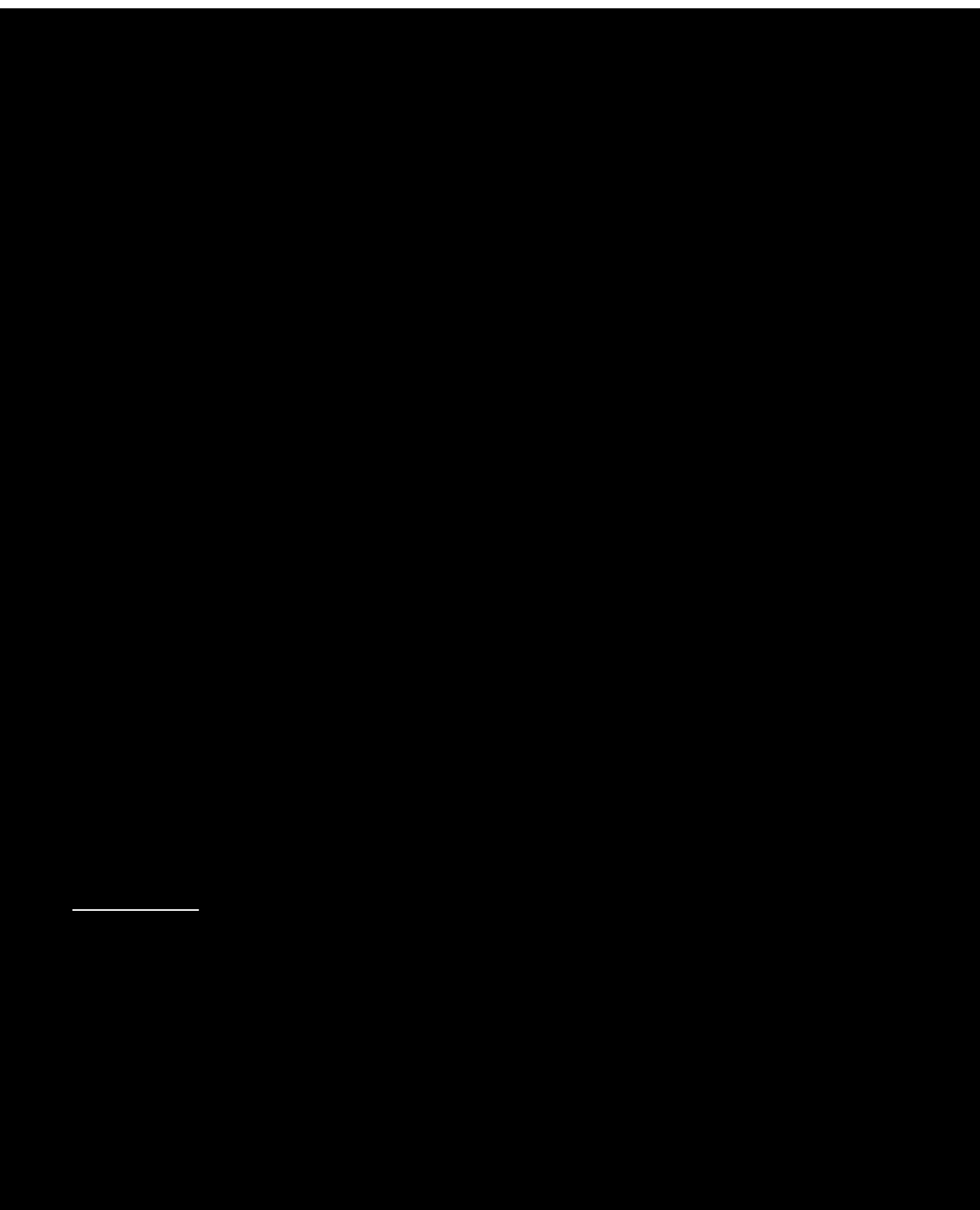
Average energy and solvent-accessible surface area differences were fit to the experimental binding data (Table 1) to obtain linear response parameters α , β , and γ according to eqs (1)–(3). This procedure was performed with a Simplex-based algorithm. As inhibition data for the majority of the ligands in this set has been reported by Holt and co-workers,^{9,10} in cases where two values have been measured the values from these authors were used for fitting.

Results and Discussion

Average intermolecular energy components and SASAs

Each ligand and protein–ligand complex was solvated with a sphere of explicit water molecules and sampled as described above. Average energy components and





Explore Litigation Insights

Docket Alarm provides insights to develop a more informed litigation strategy and the peace of mind of knowing you're on top of things.

Real-Time Litigation Alerts



Keep your litigation team up-to-date with **real-time alerts** and advanced team management tools built for the enterprise, all while greatly reducing PACER spend.

Our comprehensive service means we can handle Federal, State, and Administrative courts across the country.

Advanced Docket Research



With over 230 million records, Docket Alarm's cloud-native docket research platform finds what other services can't. Coverage includes Federal, State, plus PTAB, TTAB, ITC and NLRB decisions, all in one place.

Identify arguments that have been successful in the past with full text, pinpoint searching. Link to case law cited within any court document via Fastcase.

Analytics At Your Fingertips



Learn what happened the last time a particular judge, opposing counsel or company faced cases similar to yours.

Advanced out-of-the-box PTAB and TTAB analytics are always at your fingertips.

API

Docket Alarm offers a powerful API (application programming interface) to developers that want to integrate case filings into their apps.

LAW FIRMS

Build custom dashboards for your attorneys and clients with live data direct from the court.

Automate many repetitive legal tasks like conflict checks, document management, and marketing.

FINANCIAL INSTITUTIONS

Litigation and bankruptcy checks for companies and debtors.

E-DISCOVERY AND LEGAL VENDORS

Sync your system to PACER to automate legal marketing.